

# Photodissociation of acetaldehyde: The CH<sub>4</sub>+CO channel

Benjamin F. Gherman, Richard A. Friesner, Teh-Hwa Wong, Zhiyuan Min, and Richard Bersohn<sup>a)</sup>

*Department of Chemistry, Columbia University, New York, New York 10027*

(Received 11 August 2000; accepted 26 January 2001)

*Ab initio* quantum chemical calculations for the molecular dissociation channel of acetaldehyde are reported. The enthalpy change for the dissociation of acetaldehyde into methane and carbon monoxide was calculated to be exoergic by 1.7 kcal/mol. The transition state for this unimolecular dissociation, confirmed by normal mode analysis, was found to have an activation energy of 85.3 kcal/mol. Experimental measurements are reported for the vibrational and rotational state distribution of the CO product. No  $v=1$  CO is found and the rotational temperature is  $1300 \pm 90$  K. The reaction coordinate at the transition state implies that the CO product is vibrationally cold and rotationally hot. This conclusion, which requires quantum dynamics calculations to confirm definitively, does agree with and aids in explaining the experimental results. © 2001 American Institute of Physics. [DOI: 10.1063/1.1355983]

## I. INTRODUCTION

Formaldehyde, acetaldehyde, and acetone are the prototypes of carbonyl group photochemistry. They all exhibit a weak, very broad  $n \rightarrow \pi^*$  transition extending throughout the near UV.<sup>1</sup> Acetaldehyde, in particular, absorbs between 29 400 and 43 500  $\text{cm}^{-1}$  with  $\epsilon_{\text{max}}=12$ . Near the threshold for absorption there is an emission which in acetaldehyde begins to disappear at around 31 200  $\text{cm}^{-1}$  and is finished at 31 500  $\text{cm}^{-1}$ .<sup>2,3</sup> The decrease of the emission coincides with the onset of predissociation. The initial  $n \rightarrow \pi^*$  excitation increases the C–O bond length, makes the molecule pyramidal, and decreases the dipole moment. The interest and complexity of these three compounds arises from the fact that in the excited  $S_1$  state the weakened C–O bond is still the strongest bond in the molecule. The photochemistry must therefore be indirect, involving crossings between different potential energy surfaces. A correlation argument leads to the same conclusion. The excited state  $S_1$  of an aldehyde RCHO correlates to a hydrogen atom and an electronically excited RCO radical. The molecular pair RH and CO must be derived from the nondegenerate singlet ground state,  $S_0$ . The radical pair R+HCO can be derived from either the ground  $S_0$  or the triplet state,  $T_1$ .

The fact that dissociation to the molecular channel does not begin simultaneously with absorption implies that the molecule is slow to leave  $S_1$  and reach  $S_0$  or that in  $S_0$  there is a barrier to dissociation. However, just 3 to 4 kcal/mol above the energy threshold for the radical pair channel, fluorescence decreases and dissociation begins. Thus there is no difficulty in crossing from  $S_1$  to  $T_1$ . At these relatively low energies there is no evidence for the molecular pair channel. Let us assume that the rate of dissociation on  $T_1$  is always faster than the rate of intersystem crossing to the ground state. If so, it must follow that internal conversion from  $S_1$  to  $S_0$  is the route for forming the molecular pair. At a suffi-

ciently high energy, because of the rapidly increasing density of states, the rates of internal conversion and intersystem crossing become comparable. The quantum yields of the two channels therefore become of comparable magnitude. The quantum yield of CO+CH<sub>4</sub> does indeed rise from 0.001 at 313.0 nm to 0.15 at 280.4 nm to 0.28 at 265.4 nm to 0.66 at 253.7 nm.<sup>1</sup> At the experimentally convenient wavelength of 248.4 nm ( $42\,560\text{ cm}^{-1}$ ) the CO+CH<sub>4</sub> channel is the dominant channel.

Considerable effort has been and is being expended on the radical pair channel, CH<sub>3</sub>+HCO.<sup>2,4</sup> The present paper is devoted to the molecular channel, i.e., unimolecular dissociation of a hot ground state acetaldehyde molecule. The vibrational and rotational state distribution of the CO product of this dissociation is measured. An *ab initio* calculation computes for the ground state the correct structure of acetaldehyde, accurate vibrational frequencies, and energies of reaction. The structure, frequencies, and reaction coordinate of the transition state are calculated to provide a theoretical understanding of the quantum state distribution.

## II. EXPERIMENTAL METHOD AND RESULTS

The nascent CO resulting from the 248 nm photodissociation of CH<sub>3</sub>CHO flowing through a cell at 80 millitorr pressure was probed by a method of vacuum ultraviolet (VUV) laser induced fluorescence first introduced by Hepburn in which the  $A(^1\Pi)$  state near 154 nm is excited by laser light.<sup>5</sup> The 154 nm light is made by combining 250 and 664 nm light. The method has been described in detail in a recent paper.<sup>6</sup> The delay time between the probe laser and the photodissociation laser was 200 ns.

No vibrationally excited CO ( $v=1$ ) was detected. The logarithm of the intensities divided by the degeneracy factor ( $2J+1$ ) and corrected for the Honl–London factor are plotted in Fig. 1 against  $J(J+1)$ . The data fits roughly the straight line expected for a Boltzmann distribution at 1300 K. The standard deviation of the fit to a straight line is 90 K.

<sup>a)</sup>Electronic mail: rb18@columbia.edu

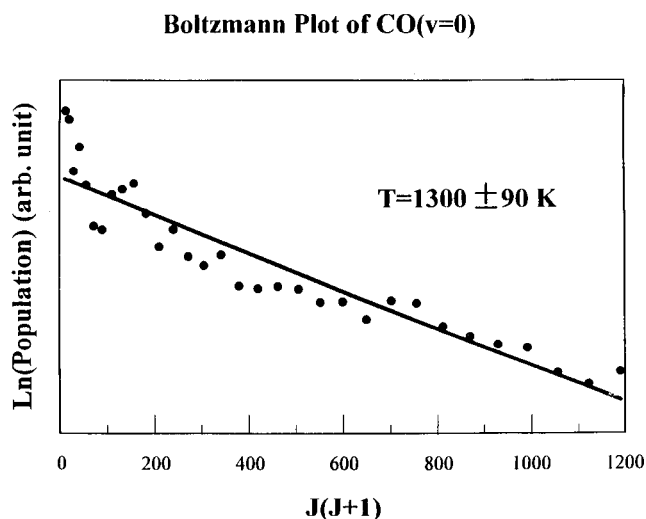


FIG. 1. Plot of  $\ln[P(J)/(2J+1)]$  vs  $J(J+1)$  where  $P(J)$  is the relative population of state  $J$ .

The laser-induced fluorescence (LIF) excitation spectrum for CO closely resembled that in Fig. 2(b) from Min and coworkers<sup>6</sup> in which CO had a similar rotational temperature to that of the present study. The LIF signal of the CO ( $v=0, J$ ) was linear in the intensity of the 248 nm laser. This is a useful but not perfect method to verify that multiphoton processes are not dominant. Finally, without the photodissociation laser there was no LIF signal. The observed CO is not a result of photodissociation of HCO by the 250 nm light accompanying the VUV probe light. In other experiments HCO has been formed in reactions and dissociated by 250 nm light but the rotational temperatures were always less than 500 K. The reason is that the departing light H atom does not exert much torque on the CO molecule.

### III. COMPUTATIONAL METHODS

Calculations were carried out with the JAGUAR version 3.5<sup>7</sup> and JAGUAR version 4.0<sup>8</sup> suite of *ab initio* quantum chemistry programs. The accuracy of the density functional theory (DFT) methods employed in JAGUAR has been documented elsewhere.<sup>9</sup> We expect the error in calculations employing the B3LYP-DFT (Refs. 10 and 11) functional to be less than 2 kcal/mol. The calculations were run as serial jobs on three types of machines: Silicon Graphics workstations running IRIX version 6.5 with 180 MHz R10k processors, IBMs running AIX version 4.1 with 200 MHz power PC 604e processors, and PCs running SOLARIS version 5.7 with 200 MHz Pentium-pro processors.

### IV. RESULTS AND DISCUSSION

#### A. Calculations for the reactant and products

The absolute energies of the reactant (acetaldehyde) and products (methane and carbon monoxide) were obtained in a three-step process. A crude geometry optimization was first performed using the Hartree-Fock (HF) method with the 6-31G\*\* basis. This structure was then refined further with DFT-B3LYP with the 6-31G\*\* basis. Both sets of geometry

TABLE I. Absolute energies and experimental heats of formation for the reactant and products.

	Absolute energy (hartrees)	Experimental heat of formation (Ref. 12)
acetaldehyde	-153.889 15	-40.798
methane	-40.537 56	-17.8951
carbon monoxide	-113.354 29	-26.4166

optimizations employed analytical gradient methods. Finally, a single-point energy calculation was performed with DFT-B3LYP with the cc-pvtz(-f) basis set. The energies calculated in this manner as well as the experimental heats of formation<sup>10</sup> are given in Table I, while the optimized structure for acetaldehyde is presented in Fig. 2.

The calculated enthalpy difference for the reaction ( $-0.002\ 69$  hartrees =  $-1.7$  kcal/mol =  $-0.073$  eV) agreed well with that determined from the heats of formation ( $-0.005\ 60$  hartrees =  $-3.5$  kcal/mol =  $-0.152$  eV). Both calculation and experiment showed the reaction to be weakly exothermic. Within the limits of the accuracy of the DFT calculations, the magnitudes of the two exothermicities are in agreement.

Vibrational frequencies for the fully optimized acetaldehyde geometry were calculated with DFT-B3LYP with the cc-pvtz(-f) basis set. These frequencies are presented and compared with experimental data in Table II.<sup>13-15</sup> The average difference between the two data sets was  $45\text{ cm}^{-1}$  per frequency, with a maximum difference of  $119\text{ cm}^{-1}$  and a minimum difference of  $2\text{ cm}^{-1}$ .

The equilibrium geometry of acetaldehyde has been determined by microwave spectroscopy of four isotopomers of acetaldehyde.<sup>16</sup> The experimental (theoretical) bond lengths were C-C 1.501 Å (1.51 Å), C-O 1.216 Å (1.20 Å), and C1-H 1.114 Å (1.11 Å) and bond angles were C-C-O 123.92° (125°) and C-C-H 117.47° (115°).

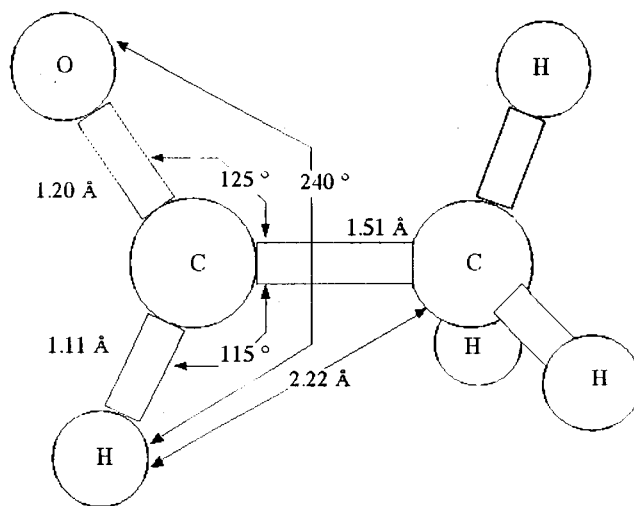


FIG. 2. Optimized geometry for acetaldehyde.

TABLE II. Vibrational frequencies (in  $\text{cm}^{-1}$ ) for acetaldehyde. Frequencies  $\nu_9$  and  $\nu_{13}$  are corrected for Fermi resonance (Refs. 14 and 15).

	Calculated	Experiment (Ref. 13)	Nature of mode	
$a'$	$\nu_1$	3118.06	3005	$\text{CH}_3$ <i>d</i> -str
$a'$	$\nu_2$	3035.58	2917	$\text{CH}_3$ <i>s</i> -str
$a'$	$\nu_3$	2868.34	2822	CH str
$a'$	$\nu_4$	1812.93	1743	CO str
$a'$	$\nu_5$	1483.28	1441	$\text{CH}_3$ <i>d</i> -deform
$a'$	$\nu_6$	1426.64	1390	CH bend
$a'$	$\nu_7$	1377.08	1352	$\text{CH}_3$ <i>s</i> -deform
$a'$	$\nu_8$	1138.57	1113	CC str
$a'$	$\nu_9$	879.79	877	$\text{CH}_3$ rock
$a'$	$\nu_{10}$	507.25	509	CCO deform
$a$	$\nu_{11}$	3106.70	2967	$\text{CH}_3$ <i>d</i> -str
$a$	$\nu_{12}$	1461.08	1420	$\text{CH}_3$ <i>d</i> -deform
$a$	$\nu_{13}$	1125.86	1107	$\text{CH}_3$ rock
$a$	$\nu_{14}$	776.72	763	CH bend
$a$	$\nu_{15}$	140.31	150	torsion

### B. Calculations for the transition state

The calculations for the transition state were carried out as a two-step process. A transition state search was first performed using DFT-B3LYP with the 6-31G\*\* basis and geometric constraints. Second, a single-point calculation of the transition state was done using DFT-B3LYP with the cc-pvtz(-f) basis set.

The transition state searches utilized two different theoretical methods. The quasi-Newton (QN) method searched for the transition state nearest to the initial geometry, by maximizing the energy along the lowest-frequency eigenvector of the Hessian and minimizing along all other coordinates. In contrast, the quadratic synchronous transit (QST) method searched for a transition state between a given reactant and product structure. The initial part of the QST-guided search was restricted to search along a circular curve connecting the reactant, transition state guess, and product. The optimizer then followed the Hessian eigenvector most similar to the tangent of the circular curve.

In the transition state searches carried out, parts of the acetaldehyde geometry not directly involved in the photodissociation (e.g., using the labels in Fig. 3, C2-O and C1-H bond lengths, H-C1-H and O-C2-C1 bond angles, and H-C1-H-H and C-C2-C1-H dihedral angles) were constrained to their values in ground state acetaldehyde. Other

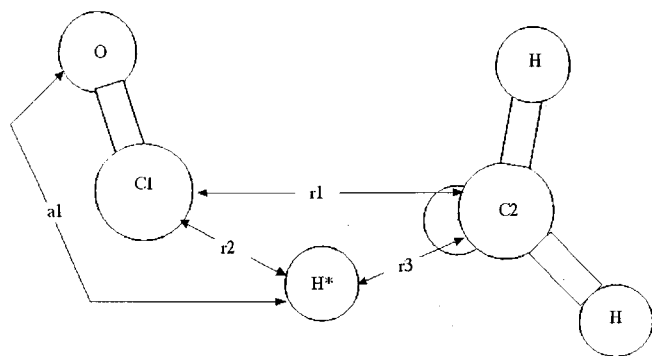


FIG. 3. Atomic labeling scheme for transition state searches and structures.

TABLE III. Geometries of the results of the transition state searches. Distances (in Å)  $r_1$ ,  $r_2$ , and  $r_3$  and angle (in degrees)  $a_1$  are defined in Fig. 2. Absolute energies are in hartree.

	Transition state result		
	No. 1	No. 2	No. 3
$r_1$	1.877	2.104	2.194
$r_2$	1.062	1.094	1.091
$r_3$	1.543	1.678	1.635
$a_1$	180.0	164.6	170.6
energy	-153.696 53	-153.696 07	-153.687 47

transition state searches had both these geometrical constraints and the requirement that the search occur strictly along the lowest bond-stretch mode in order to avoid converging to a torsional transition state in the bond-breaking reaction. One final transition state search had no constraints at all.

From the ten transition state searches, three different transition state possibilities were generated. The geometries and absolute energies (with the 6-31G\*\* basis set) of the structures are given in Table III. Normal mode analysis was done for these three structures with DFT-B3LYP and the cc-pvtz(-f) basis set (see Table IV). Only structures No. 2 and No. 3 had one negative vibrational frequency. Single-point energies for structures No. 2 and No. 3 from DFT-B3LYP calculations with the cc-pvtz(-f) basis set and the corresponding activation energies are given in Table V.

The structure with the lower energy barrier (i.e., the more optimal transition state) is structure No. 2, making this structure (Fig. 4) the “official” proposed transition state with an activation energy of 85.3 kcal/mol. Comparison of the vibrational frequencies for structures No. 2 and No. 3 shows the two sets of numbers to be very similar. One main difference is in the CO stretch frequency, which is 1816.27  $\text{cm}^{-1}$  for No. 2 and 1579.66  $\text{cm}^{-1}$  for No. 3. That the latter is rather low for a CO stretch while the former is a much more typical value provides further reason for choosing No. 2 as the optimal transition state. The value for the CO stretch

TABLE IV. Vibrational frequencies (in  $\text{cm}^{-1}$ ) for selected proposed transition state structures.

	No. 1	No. 2	No. 3	Nature of mode
$\nu_1$	3380.38	3122.52	3108.36	
$\nu_2$	3081.81	3067.63	3085.45	
$\nu_3$	3075.68	3050.80	3073.65	
$\nu_4$	2982.82	2974.16	2982.95	
$\nu_5$	1595.20	1816.27	1579.66	CO stretch
$\nu_6$	1457.08	1452.13	1451.43	
$\nu_7$	1433.09	1439.21	1438.54	
$\nu_8$	1230.15	1176.80	1129.49	
$\nu_9$	1003.53	942.67	879.37	
$\nu_{10}$	802.47	763.89	771.72	
$\nu_{11}$	708.33	571.01	570.82	
$\nu_{12}$	482.87	522.22	523.35	
$\nu_{13}$	282.75	269.57	263.54	
$\nu_{14}$	-434.76	121.87	100.64	torsion $\text{CH}_3$
$\nu_{15}$	-1563.16	-1747.89	-1827.20	reaction coordinate

TABLE V. Absolute energies for the best transition state structures and the corresponding activation energies.

	Transition state structure	
	QN-2-refine	QN-2b
energy	-153.753 23 hartrees	-153.743 86 hartrees
activation energy	0.135 92 hartrees	0.145 29 hartrees
	3.699 eV	3.953 eV
	85.29 kcal/mol	91.17 kcal/mol

for No. 2 is also much more in line with the CO stretching frequency predicted for acetaldehyde.

With an activation energy of 85.3 kcal/mol, the molecular dissociation channel should be accessible to reactant acetaldehyde having at least this much energy. Zero-point energies for optimized acetaldehyde and the transition state (structure No. 2) are 34.6 and 30.4 kcal/mol, respectively. Accounting for these zero-point energies lowers the activation energy by 4.2 kcal/mol, giving a corrected barrier of 81.1 kcal/mol and increasing the accessibility of the molecular dissociation channel to acetaldehyde.

### C. Discussion of the reaction coordinate

The motion along the reaction coordinate from the reactant to the transition state primarily involves two motions. One is the rotation of H\* from an O-C1-H\* (atom labels as defined in Fig. 3) angle of  $240^\circ$  in optimized acetaldehyde (Fig. 3) to an angle of  $165^\circ$  in the transition state (Fig. 4). The second is that as this rotation occurs, the distance between C1 and C2 increases from 1.51 Å in the reactant to 2.10 Å in the transition state. A more minor motion is the rotation of the methyl group about its central carbon atom. This rotation (Fig. 5) leads to a transition state in which the methyl group has not changed orientation relative to the carbon-oxygen bond. The methyl group is though, as a result of the rotation, poised to accept H\* from C1 as H\* continues rotating beyond the transition state and towards product.

Two other general observations are noted about the motion along the reaction coordinate. During the molecular dissociation, the CH<sub>3</sub> group does not deform to any discernible degree. Second, the carbon-oxygen bond shows a progres-

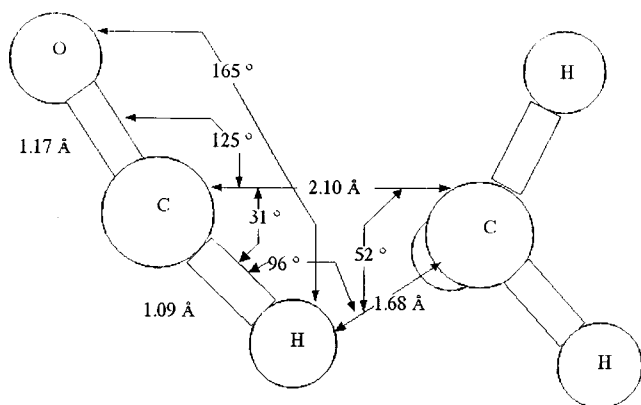


FIG. 4. Transition state geometry for molecular dissociation channel.

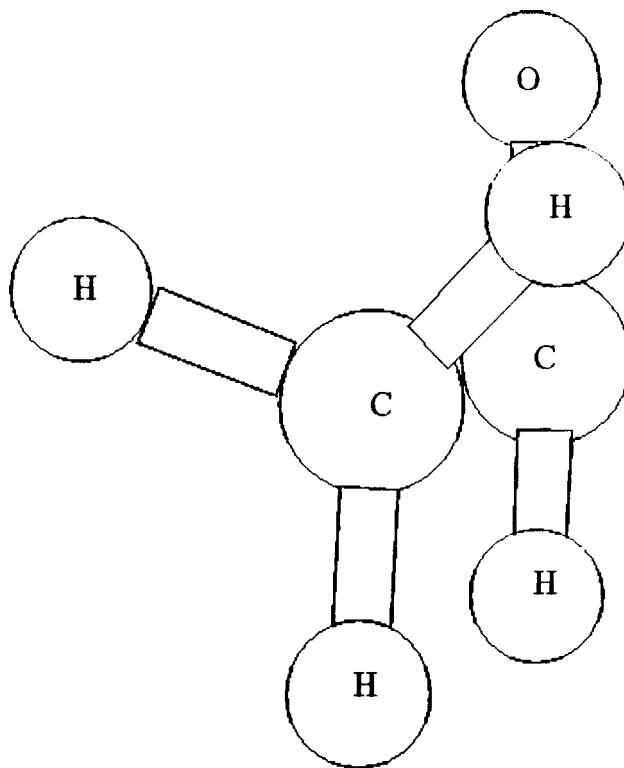


FIG. 5. Head-on view of the transition state.

sion from a double bond with a length of 1.20 Å in acetaldehyde, to having an approximate bond order of 2.5 with length 1.17 Å at the transition state, to concluding as a triple bond with length 1.13 Å in carbon monoxide.

The reaction coordinate at the transition state is illustrated in Fig. 6. The motion of H\* upon exiting the transition state is ten times greater than that of the other atoms. H\* rotates around C1 in the same manner as in its approach to the transition state except that the radius of the arc drawn by the rotation increases. The effect is that while rotating, the C1-H\* bond breaks and subsequently the C2-H\* bond forms where the awaiting empty tetrahedral site on the methyl group had been.

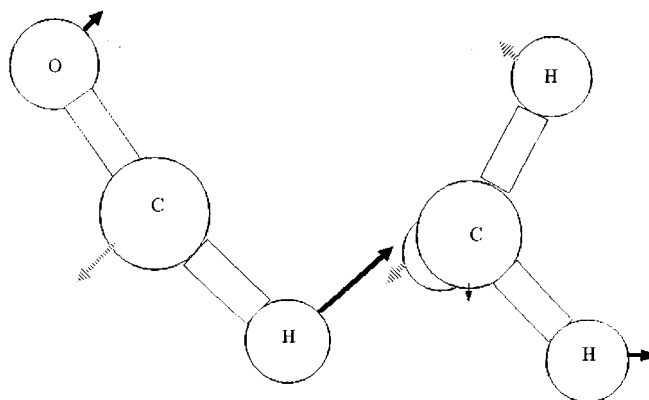


FIG. 6. Reaction coordinate for the transition state. Bold arrows represent motion out of the plane of the paper; dashed arrows, motion into the plane of the paper; and plain arrows, motion within the plane of the paper.

As  $H^*$  undergoes its motion, the burgeoning carbon monoxide rotates in a manner so that the motion of C1, which is thus necessarily opposite in direction to O, is also opposite in direction to that of  $H^*$ . While the carbon monoxide exits the reaction with this rotation, the relative constancy of the C1–O bond length indicates there is little if any vibrational excitation in the C1–O bond as a result of the reaction. Thus it is likely that the carbon monoxide produced is strongly rotating (rotationally hot) and weakly vibrating (vibrationally cold). The rotation of the carbon monoxide would center around an axis close to the oxygen atom, as a result of the motion of C1 being five times greater than that of the oxygen atom. This disparity in the motion of C1 and the oxygen atom also accounts for the translational motion of the carbon monoxide away from the newly formed methane.

In order to theoretically confirm the conjectures about the energy distribution among the rotational and vibrational degrees of freedom in the carbon monoxide produced, quantum dynamics calculations would be needed (but are beyond the means provided by JAGUAR). Nonetheless, experimental evidence (Fig. 1) does concur with this hypothesis for the energy distribution in the products. Specifically, the CO produced was found to be rotationally hot with a rotational temperature of  $1300 \pm 90$  K, and virtually all CO was found to be in the  $v=0$  state (i.e., be vibrationally cold).

The reaction can also be viewed as a pseudo two-step process. In the first step, the C1–C2 bond lengthens and breaks, creating two radicals, HCO and  $CH_3$ . The breaking of the C1–C2 bond would primarily account for the activation barrier. In the second step, the methyl radical would abstract the hydrogen atom from HCO to form  $CH_4$  plus CO. In this second step, a very weak C–H bond (energy approximately 14 kcal/mol) is exchanged for a strong C–H bond (energy approximately 90 kcal/mol). This C–H bond exchange would primarily account for the small exothermicity of the reaction.

Similar results have been reported by Yadav and Goddard based on optimization with HF and the smaller 3-21G basis set.<sup>16</sup> The transition state proposed above though shows  $H^*$  to be further rotated towards the methyl group as well as the distance between the C1 and C2 to be shorter by about 0.03 Å. The present transition state also shows less perturbation of the O–C2–C1 portion of the geometry. Activation energies reported by Yadav and Goddard calculated by single point calculations on their optimized geometry with the Möller-Plesset perturbation theory methods MP2 and MP3, singles and doubles valence shell configuration interaction (CISD) method, and CISD with size consistency correction (CISD-SSC) method and the 3-21G basis set ranged from 88 to 94 kcal/mol. Results from Belbruno,<sup>17</sup> who also arrived at a transition state highly similar to that shown in Fig. 4, indicated an activation energy of 95 to 96 kcal/mol with the QCISD method and the 6-31G\* basis set. The present result of 85.3 kcal/mol, while comparable, represents a lower barrier by 3–10 kcal/mol, making the molecular dissociation channel slightly more accessible than previously recognized.

Newer calculations by Martell, Yu, and Goddard,<sup>18</sup> however, propose a qualitatively different transition state for the

TABLE VI. Principles moments of inertia for ground state acetaldehyde and the transition state (in units of  $\text{amu} \times \text{Å}^2$ ).

	$I_a$	$I_b$	$I_c$
acetaldehyde (calculated)	8.933	49.741	55.553
acetaldehyde (experiment)	8.918	50.100	55.829
transition state (calculated)	10.099	67.700	74.599

molecular dissociation. In contrast to the geometry in Fig. 4, their new geometry has a C2– $H^*$  distance of 2.824 Å and an O–C1– $H^*$  angle of  $195.5^\circ$ . This very long C2– $H^*$  distance is argued to show that the dissociation to  $CH_4 + CO$  is a two-stage process, with HCO+ $CH_3$  as the intermediate. Calculations we have done to investigate this possibility have been unable to reproduce this result. We presently believe their transition state to be most likely that for the radical dissociation channel of acetaldehyde.

The reaction coordinate at the transition state, in addition to particular aspects of the transition state geometry, is similar to what is seen for the molecular dissociation channel of formaldehyde.<sup>19–23</sup> In both cases the C1– $H^*$  bond length remains very close to the standard C–H bond length of 1.09 Å (based on the optimized geometry for methane) at the transition state. The calculated reaction coordinate for formaldehyde indicates that the CO product is likely to be vibrationally cold and rotationally highly excited, a result much like what is predicted for the case of acetaldehyde.

#### D. Kinetics of dissociation

As a prelude to rate constant calculations for the molecular dissociation channel, the primary moments of inertia were determined for ground state acetaldehyde and the transition state (see Table VI).<sup>24</sup> Comparison of the moments of inertia for acetaldehyde between those calculated and those in the literature<sup>25</sup> was found to be excellent, with an average deviation of only  $0.217 \text{ amu} \times \text{Å}^2$ .

Using the calculated moments of inertia and the calculated vibrational frequencies for acetaldehyde and the transition state, the Rice–Ramsperger–Kassel–Marcus (RRKM) calculation of the rate constant  $k(E)$  as a function of the energy  $E$  input to the system was performed.<sup>26</sup> The RRKM calculations were done at room temperature ( $25^\circ\text{C}$ ) and vibrations were treated with the harmonic approximation. The rate constant was determined for  $E$  ranging from 81 to 205 kcal/mol in increments of 0.5 kcal/mol. Values of  $k(E)$  at some integral numbers of eV are presented in Table VII. Likewise included in Table VII is the value of  $k(E)$  (4.47

TABLE VII. Rate constant  $k(E)$  and  $1/k(E)$  for dissociation for selected values of input energy  $E$ .

$E$ (eV)	$k(E)$ (1/s)	$1/k(E)$ (s)
4.00	$1.10 \times 10^7$	$9.09 \times 10^{-8}$
5.00	$1.89 \times 10^9$	$5.29 \times 10^{-10}$
5.28	$4.47 \times 10^9$	$2.24 \times 10^{-10}$
6.00	$2.52 \times 10^{10}$	$3.97 \times 10^{-11}$
7.00	$1.30 \times 10^{11}$	$7.69 \times 10^{-12}$
8.00	$4.10 \times 10^{11}$	$2.44 \times 10^{-12}$

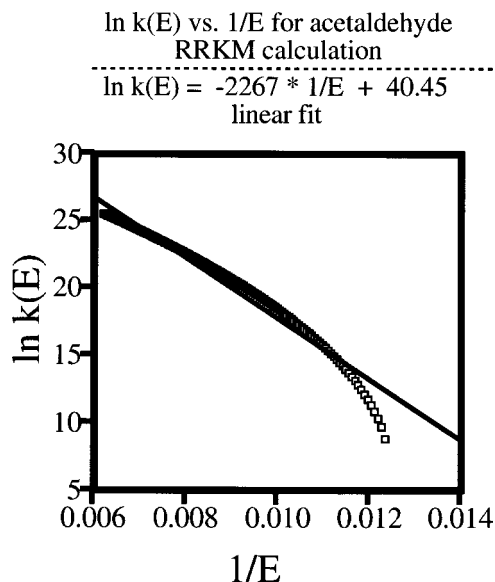


FIG. 7. Plot of  $\ln k(E)$  versus  $1/E$  using data from the RRKM calculations with the linear fit also shown.  $E$  is in units of kcal/mol.

$\times 10^9 \text{ s}^{-1}$ ) at the experimental value for  $E$  ( $42\,560 \text{ cm}^{-1} = 121.7 \text{ kcal/mol} = 5.28 \text{ eV}$ ). The time per dissociation at the experimental  $E$  is thus seen to be on the order of hundreds of picoseconds. A plot of  $\ln k(E)$  versus  $1/E$  (Fig. 7) shows the rate constant growing exponentially with the value for  $E$ . The optimal linear fit for the plot in Fig. 7 gives the approximate relation:  $\ln k(E) = -2267 \times 1/E + 40.45$ .

## V. CONCLUSION

In summary, high quality *ab initio* quantum chemical calculations have been used to study the molecular dissociation channel for acetaldehyde. The overall reaction was indicated to be exothermic by 1.7 kcal/mol from the calculations. The optimal transition state, confirmed by a normal mode calculation, had an activation energy of 85.3 kcal/mol. Most importantly, the reaction coordinate at the transition state provided strong evidence that the carbon monoxide product is vibrationally cold and rotationally hot. Experimental results presented here corroborate the predicted distribution of energy in the carbon monoxide product.

## ACKNOWLEDGMENTS

The theoretical work done by Gherman and Friesner was supported by Grant No. G40526 from the National Institutes

of Health and the experimental work of Wong, Min, and Bersohn was supported by the Chemical Sciences, Geosciences and Biosciences Division, Office of Basic Energy Sciences, U.S. Department of Energy. We acknowledge financial support from the U.S. Department of Defense through an NDSEG Fellowship to B.F.G.

- <sup>1</sup>J. G. Calvert and J. N. Pitts, Jr., *Photochemistry* (Wiley, New York, 1966), p. 369.
- <sup>2</sup>G.-H. Leu, C.-L. Huang, S.-H. Lee, Y.-C. Lee, and I.-C. Chen, *J. Chem. Phys.* **109**, 9340 (1998).
- <sup>3</sup>M. Noble and E. K. C. Lee, *J. Chem. Phys.* **80**, 134 (1984); **81**, 1632 (1984).
- <sup>4</sup>R. A. King, W. D. Allen, and H. F. Schaefer, *J. Chem. Phys.* **112**, 5585 (2000).
- <sup>5</sup>D. J. Hart and J. W. Hepburn, *J. Chem. Phys.* **86**, 1733 (1987).
- <sup>6</sup>Z. Min, R. Quandt, T.-H. Wong, and R. Bersohn, *J. Chem. Phys.* **111**, 7369 (1999).
- <sup>7</sup>JAGUAR 3.5, Schrodinger, Inc., Portland, OR, 1998.
- <sup>8</sup>JAGUAR 4.0, Schrodinger, Inc., Portland, OR, 2000.
- <sup>9</sup>R. A. Friesner, R. B. Murphy, M. D. Beachy, M. N. Ringnald, W. T. Pollard, B. D. Dunietz, and Y. Cao, *J. Phys. Chem. A* **103**, 1913 (1999).
- <sup>10</sup>B. G. Johnson, P. M. W. Gill, J. A. Pople, *J. Chem. Phys.* **98**, 5612 (1993).
- <sup>11</sup>A. D. Becke, *J. Chem. Phys.* **98**, 1372 (1993).
- <sup>12</sup>H. Y. Afeefy, J. F. Liebman, and S. E. Stein, "Neutral Thermochemical Data" in *NIST Chemistry WebBook, NIST Standard Reference Database Number 69*, edited by W. G. Mallard and P. J. Linstrom, February, 2000 (National Institute of Standards and Technology, Gaithersburg, MD, 2000), p. 20899 (<http://webbook.nist.gov>).
- <sup>13</sup>T. Shimanouchi, *Tables of Molecular Vibrational Frequencies*, Publication NSRDS, Natl. Stand. Rep. Data Serv., Natl. Bur. Stand. Circ. No. 39 (U.S. GPO, Washington, D.C., 1972).
- <sup>14</sup>H. Hollenstein and Hs. H. Gunthard, *Spectrochim. Acta, Part A* **27**, 2027 (1971).
- <sup>15</sup>H. Hollenstein, *Mol. Phys.* **39**, 1013 (1980).
- <sup>16</sup>S. Yadav and J. D. Goddard, *J. Chem. Phys.* **84**, 2682 (1986).
- <sup>17</sup>J. J. Belbruno, *J. Phys. Org. Chem.* **10**, 113 (1997).
- <sup>18</sup>J. M. Martell, H. Yu, and J. D. Goddard, *Mol. Phys.* **92**, 497 (1997).
- <sup>19</sup>C. B. Moore and J. C. Weisshaar, *Annu. Rev. Phys. Chem.* **34**, 525 (1983).
- <sup>20</sup>J. D. Goddard and H. F. Schaefer III, *J. Chem. Phys.* **70**, 5117 (1979).
- <sup>21</sup>J. D. Goddard, Y. Yamaguchi, and H. F. Schaefer III, *J. Chem. Phys.* **75**, 3459 (1981).
- <sup>22</sup>W. Chen, W. L. Hase, and H. B. Schlegel, *Chem. Phys. Lett.* **228**, 436 (1994).
- <sup>23</sup>L. M. M. de A. Martins, G. Arbilla, and E. C. da Silva, *J. Phys. Chem. A* **102**, 10805 (1998).
- <sup>24</sup>R. G. Gilbert, S. C. Smith, and M. J. T. Jordan, *UNIMOL Program Suite (Calculation Fall-off Curves for Unimolecular and Recombination Reactions)* (Sydney University, Australia, 1993).
- <sup>25</sup>R. W. Kilb, C. C. Lin, and E. B. Wilson, Jr., *J. Chem. Phys.* **26**, 1695 (1957).
- <sup>26</sup>RRKM program. Modified by M. A. Hanratty and D. V. Dearden, "Distribution by Phase Space Theory" (March 1, 1986), from W. L. Hase and D. L. Bunker, *A General RRKM Program* (California Institute of Technology, Pasadena, 1985).